Transport properties in C_{60} field-effect transistor with a single Schottky barrier

Yohei Ohta,[1] Yoshihiro Kubozono,[1,a)] and Akihiko Fujiwara[2]
[1]*Research Laboratory for Surface Science, Okayama University, Okayama 700-8530, Japan*
[2]*Japan Advance Institute of Science and Technology, Ishikawa 923-1292, Japan*

(Received 13 March 2008; accepted 15 April 2008; published online 2 May 2008)

C_{60} field-effect transistor (FET) has been fabricated with a single Schottky barrier formed by an insertion of 1-dodecanethiol at the interface between the active layer and the gate dielectric. The suppression of drain current is observed at low drain-source voltage, showing a formation of the carrier injection barrier. Furthermore, a clear difference between forward and reverse drain currents is observed in the FET in a high temperature region, showing that this FET device is close to an ideal single Schottky diode. The quantitative analysis for carrier injection barrier has been achieved with thermionic emission model for a single Schottky barrier. © *2008 American Institute of Physics*. [DOI: 10.1063/1.2919799]

Field-effect transistors (FETs) with organic molecules have been extensively studied for potential applications in next-generation electronics,[1] and they are also tested in a wide field such as nanotechnology and sensing system.[2,3] However, an operation mechanism of FET with organic molecule is still under investigation. Especially, a clarification of mechanism for carrier injection into active layer is one of the most important research subjects. Recently, carrier injection mechanism has been investigated for C_{60} and pentacene FET devices with source/drain Au electrodes modified by 1-alkanethiols ($C_nH_{2n+1}SH$) by our group.[4–6] The studies are achieved by the analyses of the observed drain current density J_D versus drain-source voltage V_{DS} plots with the theoretical formula of the thermionic emission model for double Schottky barriers,[4]

$$J_D = A^* T^2 \exp\left(-\frac{\phi_B^{\text{eff}}}{k_B T}\right) \frac{\sinh\left(\frac{eV_{DS}}{2k_B T}\right)}{\cosh\left(\frac{eV_{DS}}{2nk_B T}\right)}, \tag{1}$$

where A^*, ϕ_B^{eff}, T, n, and k_B are the effective Richardson constant, effective Schottky barrier height, elementary charge, temperature, ideality factor, and the Boltzmann constant, respectively. The ϕ_B^{eff} is given by

$$\phi_B^{\text{eff}} = \phi_B + k_B T \beta l, \tag{2}$$

where ϕ_B, β, and l refer to the Schottky barrier height of pure Au–C_{60}/pentacene junction, the tunneling efficiency of carriers, and the length of insulating layer formed by $C_nH_{2n+1}SH$, respectively. The second term in the right side of Eq. (2) is associated with the tunneling barrier. The ϕ_B and β could be determined from either temperature or length dependence of ϕ_B^{eff}.[4–6] The ϕ_B for pure Au–C_{60} junction, 0.09–0.17 eV, was quite smaller than that expected from a simple band picture, 1.5 eV.[7,8] The β value was 0.65–1.12 $Å^{-1}$ for electron and hole,[4–6] which was consistent with the value, 0.8–1.4 $Å^{-1}$, determined by scanning tunneling microscope.[9,10] Subsequently, Stoliar *et al.* studied the dependence of μ on l in the pentacene FET with two Au electrodes modified by $C_nH_{2n+1}SH$, and they found a very interesting even-odd effect of number of C atoms (n) on μ.[11]

Here, we point out a necessity of quantitative analysis of the carrier injection barrier in the organic FET device with a single Schottky barrier. In this device, only one electrode is covered with $C_nH_{2n+1}SH$; i.e., one junction of Au-active layer has a large tunneling barrier formed by $C_nH_{2n+1}SH$, and the other junction forms the Ohmic contact. The estimation of carrier injection barrier for this device can be achieved by an application of the simple theoretical model for a single Schottky barrier for the J_D-V_{DS} curve. The fabrication of this type of device is of significance to examine whether the carrier injection barrier height and tunneling efficiency determined by the thermionic emission model for double Schottky barriers[1–3] are reliable. Furthermore, an application of organic device may be found by a combination of the FET and diode properties because of an expectation of a rectifying behavior in the organic FET with a single Schottky barrier.

The device structure and measurement mode of C_{60} FET with a single Schottky barrier are shown in Figs. 1(a) and 1(b). First, a Au (18 nm) electrode was formed on the Si/SiO_2 substrate, and Cr (5 nm) was deposited as adhesion layer between Au and SiO_2. Further, this electrode was covered with $C_{12}H_{25}SH$ by immersing the substrate into 1.0×10^{-2} mol dm^{-3} $C_{12}H_{25}SH$ ethanol solution. The C_{60} thin films with thickness of 50 nm are formed on the substrate. Another Au electrode (thickness of 40 nm) was formed on the C_{60} thin films. Therefore, one electrode is bottom contact and the other is top contact for C_{60} thin films. The insulating $C_{12}H_{25}SH$ layer is formed in the interface between Au electrode and C_{60} thin films in the bottom-contact side. On the other hand, in top-contact side, Au must penetrate into the C_{60} films under the electrode. In this side, we can expect an Ohmic-like contact.

The contact angle α of water on the surface of Au electrode modified by $C_{12}H_{25}SH$ was 90°, showing a homogeneous coverage by $C_{12}H_{25}SH$. The work function ϕ_m determined from the onset of photoemission spectrum was 4.75 eV. This indicates that the surface is not Cr but Au covered with $C_{12}H_{25}SH$. The channel length and channel width were 80 and 2900 μm, respectively. The capacitance per area of SiO_2 was 8.63×10^{-9} F cm^{-2}. The channel thickness used for the estimation of J_D was taken as 2 nm based

a)Electronic mail: kubozono@cc.okayama-u.ac.jp.

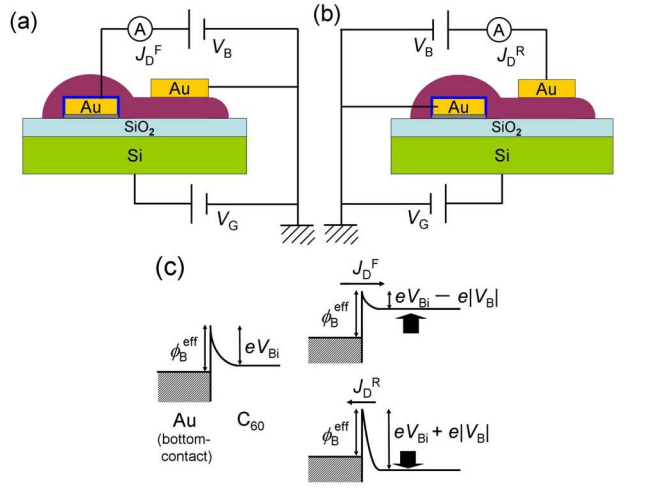

FIG. 1. (Color online) Device structure and measurement mode of C_{60} FET with a Au electrode covered with $C_{12}H_{25}SH$: (a) J_D^F measurement mode and (b) J_D^R measurement mode. The regions shown by colors of blue, gray, and purple refer to $C_{12}H_{25}SH$, Cr and C_{60} thin films, respectively. (c) Energy band diagrams for a single Schottky barrier: (left) $V_B=0$, (top of right) V_B (>0) applied to the Au electrode, and (bottom of right) V_B (>0) applied to the C_{60}.

on the previous result.[6,12] Through this letter, the forward and reverse current densities refer to J_D^F and J_D^R, respectively. The J_D^F was recorded by applying positive bias voltage V_B to bottom-contact side ($V_B=V_{DS}>0$) [Fig. 1(a)], while J_D^R was recorded by applying positive bias voltage V_B to top-contact side ($-V_B=V_{SD}<0$) [Fig. 1(b)]. Therefore, $|V_B|$ for $|J_D^F|$-$|V_B|$ curve corresponds to $|V_{DS}|$, and $|V_B|$ for $|J_D^R|$-$|V_B|$ curve refers to $|V_{SD}|$. All transport characteristics of FET were measured by increasing the absolute values of $|V_{DS}|$ (or $|V_{SD}|$) and $|V_G|$ under vacuum of 10^{-6} Torr.

The $|J_D^F|$-$|V_B|$ and $|J_D^R|$-$|V_B|$ curves ($V_G=100$ V) at 300 K are shown in Fig. 2(a). The values of $|J_D^F|$ are larger than those of $|J_D^R|$ in all $|V_{DS}|$ regions, and a nonlinear concave-up behavior is observed in both the $|J_D|$-$|V_B|$ plots. Actually, a larger nonlinear concave-up behavior is observed in $|J_D^F|$-$|V_B|$ curve than in $|J_D^F|$-$|V_B|$ curve. As seen from the energy band diagram of Au–$(C_{12}H_{25}SH)$–C_{60} junction shown in Fig. 1(c), when the positive V_B is applied to the Au electrode covered with $C_{12}H_{25}SH$ (bottom-contact electrode) [Fig. 1(a)], the potential barrier in the C_{60} films reduces from built-in potential eV_{Bi} to $eV_{Bi}-e|V_B|$. On the other hand, when the V_B is applied to the pure Au electrode (top-contact electrode) [Fig. 1(b)], the potential barrier in the C_{60} films increases from eV_{Bi} to $eV_{Bi}+e|V_B|$. This band pictures clearly explain the relationship $|J_D^F|>|J_D^R|$ under the applied V_B. Thus, a clear rectifying behavior is observed in this single Schottky diode FET device at 300 K.

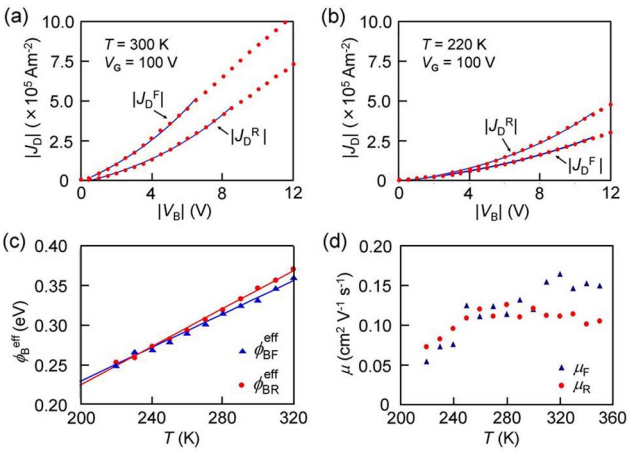

FIG. 2. (Color online) $|J_D^F|$-$|V_{DS}|$ and $|J_D^R|$-$|V_{DS}|$ plots (a) at 300 and (b) at 220 K, and (c) ϕ_{BF}^{eff}-T and ϕ_{BR}^{eff}-T plots and (d) μ_{eff}^F-T and μ_{eff}^R-T plots for C_{60} FET with a Au electrode covered with $C_{12}H_{25}SH$.

As seen from Fig. 2(b), nonlinear concave-up behaviors are more clearly observed in both $|J_D|$-$|V_B|$ curves at 220 K than those at 300 K. This is reasonably explained by the fact that the number of hot electrons, which can transfer across the barrier thermally, increases with an increase in temperature. That is, $|J_D|$ increases with an increase in temperature because of the increase in hot electrons regardless of the suppression of $|J_D|$ produced by an enhancement of ϕ_B^{eff} as expected from Eq. (2). Furthermore, the relationship $|J_D^R|>|J_D^F|$ is observed in all $|V_{DS}|$ region at 220 K [Fig. 2(b)], contrary to $|J_D^F|>|J_D^R|$ at 300 K [Fig. 2(a)]. This result cannot be explained by the energy band diagram for a single Schottky barrier [Fig. 1(c)] but by that for double Schottky-like FET, as discussed later.

The curve fittings were performed for $|J_D^F|$-$|V_B|$ and $|J_D^R|$-$|V_B|$ plots in low $|V_B|$ region below ~10 V with thermionic emission model for a single Schottky barrier to determine ϕ_B^{eff} and n values, as shown in Figs. 2(a) and 2(b). The model is given by[13,14]

$$J_D = A^*T^2 \exp\left(-\frac{\phi_B^{eff}}{k_BT}\right)\exp\left(\frac{eV_B}{nk_BT}\right)\left[1-\left(\exp\frac{-eV_B}{k_BT}\right)\right]. \quad (3)$$

The direct tunneling process, which is expressed as $\exp(-\beta l)$, is involved in this equation, in the same manner as Eq. (1). Actually, a least-squares fitting for J_D^F-V_B curve recorded in the measurement mode shown in Fig. 1(a) and that for $(-J_D^R)$-$(-V_B)$ curve recorded in the measurement-mode shown in Fig. 1(b) were performed with Eq. (3). In the curve fitting, the A^* $(=4\pi em^*k_B^2/h^3)$ was fixed at the value calculated with $m^*=1.21m_0$ reported for C_{60}[15] where m_0 is the free electron mass.

The effective Schottky barrier height ϕ_{BF}^{eff} and ideality factor n_F determined from $|J_D^F|$-$|V_B|$ curve at 300 K below $|V_B|$ of 10 V were 0.3325(9) eV and 263(8), respectively, by using Eq. (3). The ϕ_{BF}^{eff} is similar to ϕ_B^{eff}, 0.3949(7) eV, determined for the C_{60} FET with two Au electrodes covered with $C_{12}H_{25}SH$.[6] However, the n_F is extremely larger than the ideal value, i.e., unity, for Schottky diode, indicating that this model is not strictly applicable for the $|J_D^F|$-$|V_B|$ curve in C_{60} FET used in this study, and the observed $|J_D^F|$ is more suppressed than the $|J_D^F|$ expected for the ideal Schottky diode.

The effective Schottky barrier height ϕ_{BR}^{eff} and ideality factor n_R determined from $|J_D^R|$-$|V_B|$ curve at 300 K were 0.347(2) eV and 1.0039(2), respectively. The ϕ_{BR}^{eff} is also similar to the value 0.3949(7) eV, for the C_{60} FET with double carrier injection barrier heights formed by $C_{12}H_{25}SH$.[3] Furthermore, the n_R is close to unity, and the value is close to 1.006(1) determined for C_{60} FET with double carrier injection barrier heights. This implies that $|J_D^R|$-$|V_B|$ curve can be reasonably analyzed with a single Schottky model [Eq. (3)]. From the difference in transport characteristics between $|J_D^F|$-$|V_B|$ and $|J_D^R|$-$|V_B|$ curves, we can indicate that a complete Ohmic contact is not still formed in

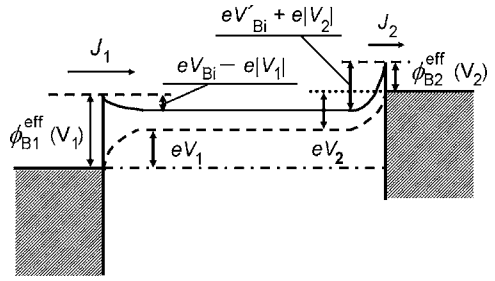

FIG. 3. Energy band diagram for double Schottky barriers ($\phi_{B1} > \phi_{B2}$ and $V_{Bi} > V'_{Bi}$). V_B ($=V_1+V_2>0$) is applied to the electrode of left side, while the electrode of right side is grounded.

C_{60}–Au junction at the top-contact side. In this case, as seen from Fig. 3, an enhancement in J_1 in the left side (bottom contact side) should be suppressed by a convergence of J_2. Here, the J_D can be derived with relationship $J_D=J_1=J_2$. Actually, when $\phi_{B1}^{\text{eff}} \gg \phi_{B2}^{\text{eff}}$, the J_D can be substantially expressed by Eq. (3) (not Eq. (1)). Nevertheless, small but nonvanishing ϕ_{B2}^{eff} ($\phi_{B1}^{\text{eff}} > \phi_{B2}^{\text{eff}}$) should lead to smaller $|J_D^F|$ than the $|J_D^F|$ expected for an ideal single Schottky diode. On the other hand, the observed $|J_D^R|$ is close to that expected for an ideal single Schottky diode because the n_R is close to 1. This can also be explained by the scenario that the $|J_D^R|$ is substantially governed by the large $eV_{Bi}+e|V_B|$ in the Au–$(C_{12}H_{25}SH)$–C_{60} junction (bottom-contact side) and that the small ϕ_{B2}^{eff} in top-contact side scarcely affects $|J_D^R|$. This led to a reasonable analysis for $|J_D^R|$-$|V_B|$ curve with a single Schottky model [Eq. (3)]. Actually, the reasonable ϕ_B^{eff} values are estimated from both $|J_D^F|$-$|V_B|$ and $|J_D^R|$-$|V_B|$ curves, i.e., $\phi_{BF}^{\text{eff}} \sim \phi_{BR}^{\text{eff}}$. This is in contrast to the fact that the n is much sensitive to the characteristics of $|J_D^F|$-$|V_B|$ and $|J_D^R|$-$|V_B|$ curves.

The ϕ_{BF}^{eff}-T and ϕ_{BR}^{eff}-T plots are shown in Fig. 2(c). These plots show linear relationship as expected from Eq. (2). Both plots showed almost the same values, indicating that the ϕ_B^{eff} are scarcely affected by an existence of small Schottky barrier in the top-contact side. Especially, the values are consistent to each other at low temperature region. The ϕ_B and β values can be determined, respectively, from the intercept and slope of the linear relations in ϕ_{BF}^{eff}-T and ϕ_{BR}^{eff}-T plots. The ϕ_B and β determined from ϕ_{BF}^{eff}-T plot were 0.026(7) eV and 0.82(2) Å^{-1}, respectively, while the ϕ_B and β from ϕ_{BF}^{eff}-T were −0.020(6) eV and 0.97(2) Å^{-1}. The β value of 0.82–0.97 Å^{-1} is close to 0.65 Å^{-1} determined for C_{60} FET with double Schottky barriers with $C_{12}H_{25}SH$.[3] On the other hand, the ϕ_B of −0.020 to 0.026 eV determined from both ϕ_B^{eff}-T plots was smaller than 0.152(4) eV for the C_{60} FET with double Schottky barriers formed by $C_{12}H_{25}SH$.[6] The small ϕ_B anyhow suggests that the Schottky barrier height is much smaller than that expected from the band diagram, 1.5 eV.[7,8]

Finally, we have estimated the field-effect mobility $\mu_F(T)$ from the square root of forward drain-saturation current $|I_{DF}^S|^{1/2}$-$|V_G|$ plot and the field-effect mobility $\mu_R(T)$, from the square root of reverse drain-saturation current $|I_{DR}^S|^{1/2}$-$|V_G|$ plot at $|V_{DS}|=100$ V. A clear difference between $\mu_F(T)$ and $\mu_R(T)$ is observed above 300 K as seen from Fig. 2(d). This implies that the rectifying effect is clearly observed in high temperature region. On the other hand, the clear rectifying behavior is not observed below 300 K. In other words, the Schottky barrier height in Au–C_{60} junction in top-contact side cannot be neglected below 300 K and this FET reaches a double Schottky like. In conclusion, a rectifying behavior (or diode property) has been observed in the C_{60} FET with a bottom-contact Au electrode covered with $C_{12}H_{25}SH$ and a top-contact Au electrode. This result verifies that this device structure is an effective and simple one for the fabrication of organic FET devices exhibiting diode property. This observation of diode property is a significant step to develop functional FET devices, which combine the FET and diode properties. From the consistency of the β, ϕ_B^{eff}, and ϕ_B values determined for the Au–$(C_{12}H_{25}SH)$–C_{60} junction in a single Schottky C_{60} FET by a simple thermionic emission model with those of C_{60} FET with double Schottky barriers determined by thermionic emission model for double Schottky barriers,[6] the thermionic emission model for double Schottky barriers[4–6] has been confirmed to be effective to an analysis of double carrier injection barriers.

This work was partly supported by a Grant-in-Aid (No. 18340104) from MEXT, Japan.

[1] C. D. Dimitrakopoulos and P. R. L. Malenfant, Adv. Mater. (Weinheim, Ger.) **14**, 99 (2002).
[2] M. Cavallini, P. Stoliar, J.-F. Moulin, M. Surin, P. Leclère, R. Lazzaroni, D. W. Breiby, J. W. Andreasen, M. M. Nielsen, P. Sonar, A. C. Grimsdale, K. Müllen, and F. Biacarini, Nano Lett. **5**, 2422 (2005).
[3] L. Torsi and A. Dodabalapur, Anal. Chem. **75**, 381A (2005).
[4] T. Nagano, M. Tsutsui, R. Nouchi, N. Kawasaki, Y. Ohta, Y. Kubozono, N. Takahashi, and A. Fujiwara, J. Phys. Chem. C **111**, 7211 (2007).
[5] N. Kawasaki, Y. Ohta, Y. Kubozono, and A. Fujiwara, Appl. Phys. Lett. **91**, 123518 (2007).
[6] Y. Ohta, N. Kawasaki, R. Nouchi, Y. Kubozono, and A. Fujiwara (unpublished).
[7] N. Hayashi, H. Ishii, Y. Ouchi, and K. Seki, J. Appl. Phys. **92**, 3784 (2002).
[8] M. Shiraishi, K. Shibata, R. Maruyama, and M. Ata, Phys. Rev. B **68**, 235414 (2003).
[9] L. A. Bamm, J. J. Arnold, T. D. Dunbar, D. L. Allara, and P. S. Weiss, J. Phys. Chem. B **103**, 8122 (1999).
[10] Y. Yasutake, Z. Shi, T. Okazaki, H. Shinohara, and Y. Majima, Nano Lett. **5**, 1057 (2005).
[11] P. Stoliar, R. Kshirsagar, M. Massi, P. Annibale, C. Albonetti, D. M. de Leeuw, and F. Biscarini, J. Am. Chem. Soc. **129**, 6477 (2007).
[12] T. Miyadera, M. Nakayama, and K. Saiki, Appl. Phys. Lett. **89**, 172117 (2006).
[13] Y. J. Liu and H. Z. Yu, J. Phys. Chem. B **107**, 7803 (2003).
[14] E. J. Faber, L. C. P. M. de Smet, W. Olthuis, H. Zuilhof, E. J. R. Sudhölter, P. Bergveld, and A. van den Berg, ChemPhysChem **6**, 2153 (2005).
[15] N. Troullier and J. L. Martins, Phys. Rev. B **46**, 1754 (1992).